Study of Surface Morphology Effects on Hg Sorption−Desorption Kinetics on Gold Thin-Films

ARTICLE *in* THE JOURNAL OF PHYSICAL CHEMISTRY C · JANUARY 2012

Impact Factor: 4.77 · DOI: 10.1021/jp2091895

4 AUTHORS, INCLUDING:

Ylias Sabri
RMIT University
49 PUBLICATIONS **284** CITATIONS
SEE PROFILE

James Tardio
RMIT University
98 PUBLICATIONS **725** CITATIONS
SEE PROFILE

Suresh Bhargava
RMIT University
431 PUBLICATIONS **3,703** CITATIONS
SEE PROFILE

THE JOURNAL OF PHYSICAL CHEMISTRY C

ARTICLE

pubs.acs.org/JPCC

Study of Surface Morphology Effects on Hg Sorption−Desorption Kinetics on Gold Thin-Films

Ylias M. Sabri, Samuel J. Ippolito,* James Tardio, and Suresh K. Bhargava*

Advanced Materials and Industrial Chemistry Group, School of Applied Sciences, RMIT University, GPO Box 2476V, Melbourne, VIC, 3001, Australia

Supporting Information

ABSTRACT: Mercury (Hg) vapor sorption and desorption kinetics on gold (Au) thin-films of different surface morphologies and at various operating temperatures have been studied by using the quartz crystal microbalance (QCM) technique. The QCM data was used to estimate Hg desorption activation energy (E_a) from Au nanostructured surfaces deposited over optically polished (Au-polished) and mechanically roughened (Au-rough) quartz substrates to better understand Hg adsorption and desorption processes, with the ultimate aim of developing better materials for Hg measurement and/or capturing applications. After accounting for the difference in active surface area, the Au-polished sample was calculated to have a Hg uptake of ∼1030 ng·cm^{-2} when exposed to 10.55 mg·m^{-3} of Hg vapor for 1 h. In comparison, the Au-polished film had a Hg uptake 15% higher than that of the Au-rough film at an operating temperature of 28 °C. However, at 132 °C, the difference increased to ∼140% higher uptake for the Au-polished film, thus indicating that each surface exhibits a different Hg−Au sticking probability which is temperature dependent. In the case of the desorption process, it was found that a higher energy is required to release the Hg from the Au-rough surface compared to that of the Au-polished surface, per unit of surface area. The mechanism was found to initially be first order for the adsorbed Hg atoms at the surface and thereafter a second-order kinetic where the absorbed/diffused Hg atoms from the bulk of the film are released.

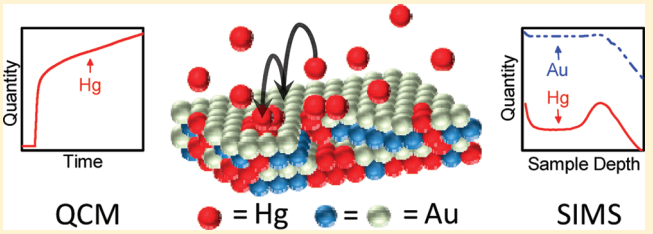

1. INTRODUCTION

Mercury being an ubiquitous environmental toxin,[1] its adverse effects on human health (i.e., lungs, heart, nervous system, etc.) have been well established[2] and have resulted in the introduction by many governments worldwide of policies that limit mercury emissions from industrial activities.[3,4] To regulate the emission of this poisonous gas, small and robust gas sensors are desirable, which can be economically installed at various locations within industrial processes. Consequently, an increased interest to develop high capacity Hg vapor sorbent materials for monitoring[5] and removing[6] Hg from a variety of different commercial and industrial applications has arisen. Materials such as Ag, Au, Pd, Pt, Al, Zn, Se, MnO_2, $PdCl_2$, Pd/polypyrrole, hopcalite, and even fine dust collected by a hot gas filter have been used to collect and/or detect airborne Hg vapor.[5−16] From among the range of sorbent materials, Schroeder et al.[17] showed metallic Au to be most commonly used as collector of Hg from ambient air, as it collects a detectable amount of mercury in a reasonable time. Metallic Au readily adsorbs and retains Hg at low temperatures but can be made to release it quantitatively following high annealing temperatures of 150−700 °C without undergoing distillation as in the case of materials with lower boiling temperatures (i.e., Ag).[17−19] Furthermore, past studies have also confirmed that the surface morphology is a critical factor when looking at adsorption and desorption behavior of Hg vapor from Au thin-films.[20,21] These studies have shown that smooth Au surfaces adsorb elemental Hg while a relatively rougher, more porous film promotes mercury diffusion into the films' grain boundaries. Our studies[22−24] of Hg interaction with Au thin-films revealed that the affinity (sticking probability) of Au deposited on an optically polished (Au-polished) substrate toward Hg decreased significantly faster than that deposited on mechanically roughened (Au-rough) substrate when exposed to Hg vapor.[24] These results agreed well with previous studies[21,25−27] where it was proposed that the higher affinity of the Au-rough surface toward Hg vapor was due to the Hg diffusion into the films' bulk, thus resulting in the release of surface adsorption sites and promoting further Hg sorption to occur at the surface. Despite the numerous studies involving Hg vapor sorption on Au films, the sorption/amalgamation process between these two metals is not well understood, reportedly because of the ease of the amalgamation process.[28−30] Additionally, to the best of our knowledge, literature concerning the regeneration of Au thin-films upon desorption of Hg amalgam is limited to two reports.[29,31] Therefore, the impetus for this study is to better understand Hg sorption with more emphasis on Hg desorption behavior from Au thin-films for sensing applications.

A significant application of Au thin-films is to employ them as chemically sensitive layers in transducer-based Hg vapor sensors such as the conductometric-[8] and acoustic[32,33]-based sensors. One such transducer platform is the quartz crystal microbalance

Received: September 23, 2011
Revised: December 1, 2011
Published: December 08, 2011

(QCM), which is an example of a mass-based transducer that has successfully been demonstrated as a potential mercury vapor sensor.[33] Because of their high sensitivity ($ng \cdot cm^{-2} \cdot Hz^{-1}$), such devices have also been used to study solid/fluid interfaces such as the investigation of thin-film surfaces toward fluid sorption, chemical deposition, dissolution, molecular recognition, etching studies, estimation of stress effects, and many other chemical and physical processes.[34−37] The QCM technique utilizes the linear relationship between the frequency shift (Δf) and the mass change (Δm) observed on the electrode surface given by:

$$\Delta f = -\frac{2f_0^2}{A\sqrt{\mu_q \rho_q}}\Delta m = -S_f \Delta m \quad (1)$$

where S_f represents the integral mass sensitivity (or Sauerbrey constant) and is proportional to the square of the fundamental frequency (f_0) and inversely proportional to the active surface area (A) of the QCM electrode.[37] The quartz crystal density (ρ_q) and shear modulus (μ_q) are 2.648 $g \cdot cm^{-3}$ and 2.947×10^{11} $g \cdot cm^{-1} \cdot s^{-2}$, respectively.[38]

In this study, the Hg sorption/desorption kinetics from Au thin-films are experimentally obtained by using the relationship between QCM response and mass sorption/desorption as in eq 1 following Hg exposure of the Au films under controlled conditions. The activation energy is then calculated as a function of time $\{E_a(t)\}$ from the derivative of the QCM response curves when exposed to Hg vapor at various operating temperatures. These calculations are performed for both the Au-polished and Au-rough thin-films to compare and gain a better understanding of the interaction between Au thin-films of different morphology and Hg vapor.

2. EXPERIMENTAL SECTION

2.1. QCM Fabrication. Two similar sized 10 MHz QCM resonators, one of which had optically polished quartz crystal faces and the other had mechanically roughened faces, were purchased from Hy-Q Crystals, Victoria, Australia. The QCM electrodes were formed by depositing a 100 nm thin-film of Au over a 10 nm Ti adhesion layer (at a rate of 0.2 nm/s) on both faces of the quartz crystals by a Balzers e-beam (BAK 600) evaporator at room temperature (~22 °C). A base pressure of 1.5×10^{-7} Torr was used prior to deposition. Both the optically polished and mechanically roughened quartz crystal substrates were coated using the same deposition conditions so that the morphological characteristics of the deposited gold film were only influenced by the underlying topology of the chosen quartz crystal substrates.

Additionally, to better understand the diffusion behavior of Hg in Au films, a specially designed ultrathin (40 nm) Au film-based QCM was also fabricated and exposed to Hg vapor so that it could be characterized using secondary ion mass spectroscopy (SIMS) depth profiling. The 40 nm Au film was deposited directly on the Au electrode of the QCM with a 40 nm thick SiO_2 barrier layer sandwiched between the two Au films (i.e., Au electrode of the QCM and the 40 nm Au ultrathin film) to stop further diffusion of Hg beyond the 40 nm ultrathin film and through the Au electrode.

2.2. Hg Exposure and Monitoring. Mercury vapor concentrations were achieved by using mercury permeation tubes which were purchased from VICI, Houston, TX. Different Hg concentrations were generated using a PID temperature controller at different set points to heat the permeation tubes. Each Hg concentration was calibrated using acidic a $KMnO_4$ wet trapping method, which was adapted from the Ontario Hydro method.[16,39] The Hg trapped in the $KMnO_4/H_2SO_4$ solution was quantified by inductively coupled plasma mass spectroscopy using an Agilent Technologies HP4500 series 300 ShieldTorch system.

The change in resonant frequency (Δf) of the QCMs was measured using a Maxtek RQCM (10 MHz phase-locked oscillator, Beaverton, OR) with a resolution of ±0.01 Hz. Each QCM was tested toward five Hg concentrations of 1.02, 1.87, 3.65, 5.70, and 10.55 $mg/m^3 \pm 0.05$ mg/m^3 (balance N_2) in increasing order using 1 h exposure times for each Hg concentration (unless else specified). When combined with a 1 h recovery period of dry N_2, each 1 h Hg exposure period and 1 h recovery period is referred to as a pulse throughout this manuscript. The sensors were exposed to a pulse sequence with increasing Hg concentration at each of the nine tested operating temperatures which started at 132 °C and decreased to 28 °C ± 1 °C over eight decrements of ~13 °C. In between each operating temperature change, the sensors were held under a continuous flow of dry N_2 for the sensors to stabilize. The gas flow rate into the chamber was kept constant at 200 sccm using a custom-built four-channel mass flow controller system, maintaining a constant pressure of 1200 Torr throughout the entire experiment. The approximate volume of the chamber housing the QCM sensors was ~0.5 L. The Hg accumulated between each Hg pulse was taken into consideration when calculating Hg sorption and desorption kinetics at the tested operating temperatures from the differences in the QCM response during Hg sorption and recovery parts of each pulse.

The specially designed ultrathin Au film-based QCM was exposed to a Hg vapor concentration of 10.55 mg/m^3 for a period of 14 h before being flushed by dry N_2 for 5 h at an operating temperature of 28 °C. The purpose of the 5 h recovery period was to remove any loosely attached Hg atoms from the surface of the Au ultrathin film-based QCM prior to removing the device from the gas chamber. Thereafter, the QCM was stored for 30 days before being analyzed by SIMS depth profiling.

2.3. Surface Characterization. Scanning electron microscope (SEM) characterization was performed using a FEI Nova SEM instrument operating at an accelerating voltage of 10 kV, spot size of 3, and working distance of 4.5 mm.

X-ray diffraction (XRD) data was obtained with a Bruker D8: Discover which employed a General Area Detector Diffraction System (GADDS) using a Cu Kα radiation (wavelength 1.5418 Å) source operating at 40 kV and 40 mA and a 0.5 mm colorimeter. The detector data collection range was ±15° from each of the fixed detector locations using 2θ values of 25°, 55°, and 70° and ω values of 12.5°, 27.5°, and 35°. Each scan was performed for a total of 30 min (10 min at each position) to collect the diffraction peaks for each sample.

Secondary ion mass spectroscopy (SIMS) was performed on a Cameca IMS 5f instrument. SIMS depth profiles were performed using a Cs^+ primary ion beam of 3 keV net impact energy, a 1.5 nA beam current, and a raster area of 500 × 500 μm. To eliminate potential edge effects, a combination of lens settings was used to restrict the secondary ion yield to a 100 μm diameter region within the center of the raster area.

To determine the electrochemical surface area (ESA) of Au thin-films, experiments were conducted at ~20 °C with a CH Instruments (CHI 760C) electrochemical analyzer in an electrochemical cell (BAS) that allowed reproducible positioning of the working, reference, and counter electrodes and a nitrogen inlet tube. The Au thin-films used as the working electrode were

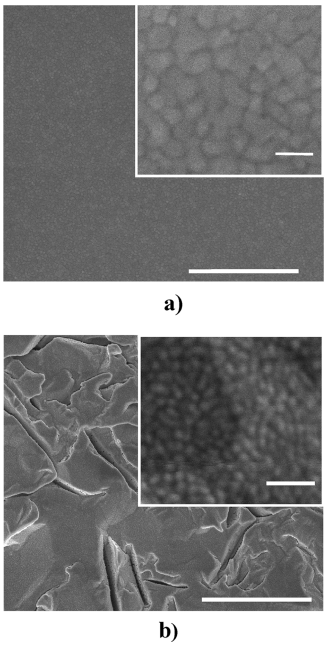

Figure 1. SEM images of (a) Au-polished and (b) Au-rough quartz crystal surfaces. Scale bars on the main and inset images represent 2 μm and 100 nm, respectively.

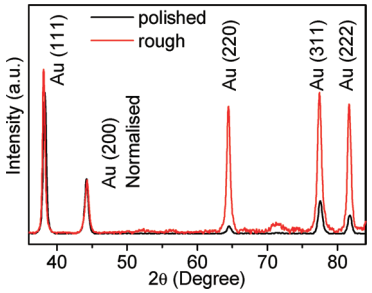

Figure 2. XRD spectra of Au-polished and Au-rough surfaces.

sonicated, washed in acetone and then methanol, and finally dried using dry nitrogen. The platinum (BAS) electrode was polished with an aqueous 0.3 μm alumina slurry on a polishing cloth (Microcloth, Buehler), sonicated in water, and dried with nitrogen. The reference electrode was Ag/AgCl (aqueous 3 M KCl). All electrochemical procedures commenced after degassing the electrolyte solutions with nitrogen for at least 10 min prior to any measurement.

3. RESULTS AND DISCUSSIONS

3.1. Surface Morphology. The SEM micrographs of the Au deposited on optically polished (Au-polished) and mechanically roughened (Au-rough) quartz substrates are shown in Figure 1a and Figure 1b, respectively. The Au-polished sample is shown to have large gold grain sizes (~80 nm), whereas the roughened substrate has much smaller gold grains (~10 nm) which are postulated to have formed from the many smaller gold grains that follow the topology of the underlying roughened quartz substrate. The AFM images (see Supporting Information, Figure S1) from a 250 nm × 250 nm scan size shows that the Au-rough surface

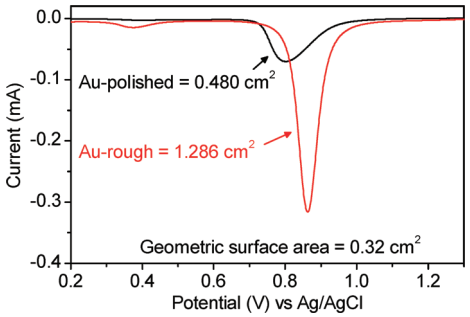

Figure 3. Electrochemical surface area of Au-polished and Au-rough quartz crystal surfaces.

has 1 order of magnitude higher roughness (average, R_a, and root-mean-square, R_q) compared to that of the Au-polished surface. The respective XRD spectra for Au-polished and Au-rough surfaces are shown in Figure 2. It is observed that the Au-polished and Au-rough surfaces have different crystalline features with the Au-rough being oriented more in the (222), (220), and (311) planes.

3.2. Electrochemical Surface Area (ESA). Prior to Hg vapor exposure of the Au QCM electrode surfaces, their electrochemical surface area (ESA) was determined by calculating the charge required for reducing the monolayer of oxide as described by Rand and Woods.[40] The integration of the cyclic voltammetric response region is shown in Figure 3. The measured electrochemical/geometrical surface area ratio of the Au-polished and Au-rough were found to be ~1.5 and 4.0 cm^2/cm^2, respectively. The flat geometric surface area was calculated to be ~0.32 cm^2 given that the diameter of both the front and back QCM electrodes were 4.5 mm each. Therefore, the Au-rough is expected to produce a response magnitude larger than that of the Au-polished-based QCM when it is exposed to the same Hg vapor concentration, mainly due to its 1.66 times higher surface area. For this reason, the ESA was used to account for the different surface areas of the Au-polished and Au-rough films when using the Sauerbrey equation, eq 1.

3.3. Hg Sorption and Desorption Kinetics. The dynamic response of the Au-polished and Au-rough QCM devices toward pulses of 1.02, 1.87, 3.65, 5.70, and 10.55 mg/m^3 of Hg vapor at an operating temperature of 28 °C are shown in Figure 4a. It can be seen that the Au-rough QCM exhibits a higher response magnitude toward Hg vapor compared to the Au-polished QCM. As expected, the Au-rough QCM was found to have a significantly higher sensitivity of 71.3 $Hz/(mg/m^3)$ as well as a better lower detection limit of 12 $\mu g/m^3$. In comparison, the sensitivity and lower detection limit of the Au-polished QCM was calculated to be 28.8 $Hz/(mg/m^3)$ and 35 $\mu g/m^3$, respectively. However, once both QCMs were normalized for their ESA (Figure 4b), both QCMs showed a similar amount of Hg having undergone sorption and desorption per square centimeter of gold film with only a marginal difference in response kinetics at the highest Hg vapor concentration of 10.55 mg/m^3 when compared to that of 1.02 mg/m^3. The difference in Hg sorption and desorption kinetics is further demonstrated in Figure 4c and Figure 4d. In Figure 4c, the first 2 min of the sensor response during a 5.70 mg/m^3 Hg pulse shows the trend of the initial rate of Hg sorption to be higher for the Au-polished QCM. This trend was observed for all tested Hg vapor concentrations and operating temperatures. Figure 4d shows the Hg sorption and desorption rate for the

dx.doi.org/10.1021/jp2091895 |J. Phys. Chem. C 2012, 116, 2483–2492

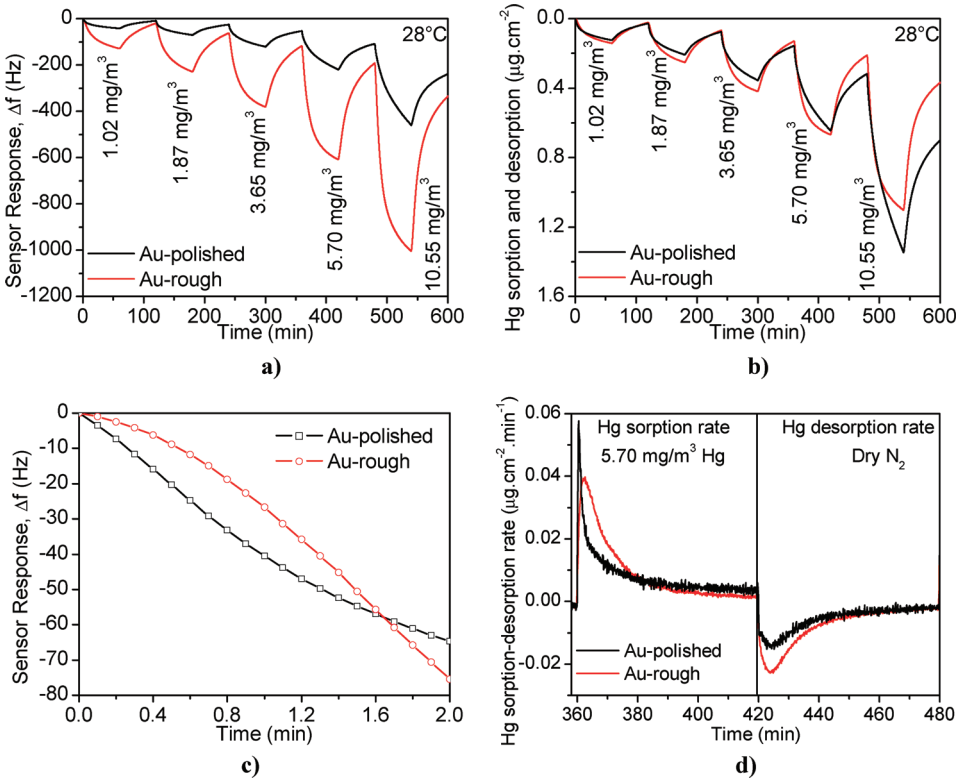

Figure 4. QCM response of (a) Au-polished and Au-rough surfaces toward various Hg vapor concentrations at 28 °C, (b) Hg sorption and desorption, (c) sensor response for Hg sorption toward a Hg vapor concentration of 5.7 mg/m^3 in the first 2 min for each QCM, and (d) Hg sorption and desorption rates during a 5.7 mg/m^3 Hg pulse. The data shown in plots b and d are normalized for the ESA of both surfaces.

5.70 mg/m^3 Hg pulse after accounting for ESA of each surface and the conversion of the sensor response to the Hg uptake (during the 1 h exposure) and release (during the 1 h recovery) period. It is shown that upon Hg exposure, the Au-polished surface reaches a higher maximum for the Hg sorption rate compared to that of the Au-rough surface; however, the maximum for the Hg desorption rate is found to be higher for the Au-rough surface during the recovery period.

To determine the Hg sorption and desorption behavior at different temperatures, the Hg exposure sequence shown in Figure 4a was performed at each of the nine tested operating temperatures. The sensor responses from the 10.55 mg/m^3 Hg pulses at the different operating temperatures are presented in Figure 5a. The temperature profiles for the two gold surfaces exhibit different trends for the response magnitudes (at a given Hg concentration) of the Au-polished and Au-rough QCMs, following a cubic and asymptotic type temperature profile, respectively. This is a clear indication of dissimilar Hg sorption kinetics between the two surface types over the range of operating temperatures tested. The temperature profiles were observed to be repeatable (see Supporting Information, Figure S2) when tests were repeated using a separate 100 nm Au-polished QCM. Furthermore, the temperature profiles of a 150 and 200 nm-based Au-polished QCM were also obtained and found to follow a trend and magnitude similar to that of the 100 nm Au-polished QCM (Figure S2). These Au thicknesses were chosen, as they are commonly used when studying mercury interaction with gold surfaces as well as for mercury monitoring applications.[26,41] Our observations indicate that Hg sorption kinetics only deviate significantly when Au films are reduced

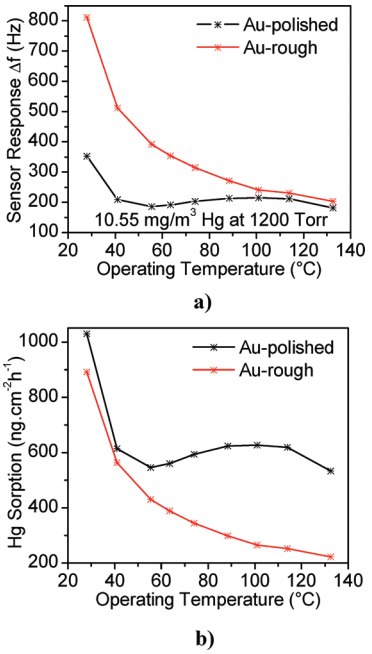

Figure 5. (a) Sensor response and (b) Hg sorption of Au-polished and Au-rough films at nine different operating temperatures ranging between 28 and 132 °C when exposed to a Hg vapor concentration of 10.55 mg/m^3 for 1 h at a constant operating pressure of 1200 Torr. The Hg sorption shown in panel b is normalized for the ESA of each film.

to 50 nm in thickness (see Supporting Information, Figure S3). Furthermore, it is quite clear from the Au-polished and Au-rough

dx.doi.org/10.1021/jp2091895 |J. Phys. Chem. C 2012, 116, 2483–2492

Table 1. Parameters *a*, *b*, and *c* at Different Operating Temperatures during Hg Desorption for Au-Polished and Au-Rough Films following Exposure to 5.7 mg/m^3 Hg[a]

	28 °C	42 °C	55 °C	63 °C	74 °C	89 °C	101 °C	114 °C	132 °C
				Au-Polished Film (5.7 mg/m^3 Hg desorption)					
a (min)	2.60	2.93	2.94	3.18	2.95	2.36	1.78	1.32	1.03
b(mol·min) × 10^{-8}	8.49	8.03	8.13	8.94	8.60	7.27	5.40	3.79	2.65
c(mol) × 10^{-11}	87.7	53.1	26.1	−4.71	−33.9	−43.6	−39.5	−20.7	−19.1
				Au-Rough Film (5.7 mg/m^3 Hg desorption)					
a (min)	19.5	21.1	19.8	17.4	15.0	13.5	13.4	11.9	12.4
b(mol·min) × 10^{-8}	34.9	28.2	19.9	16.0	12.2	10.1	9.21	7.43	7.33
c(mol) × 10^{-11}	140	54.6	−52.7	−68.3	−84.0	−35.7	−38.7	−8.72	−27.7

[a] The ESA have been accounted for when converting sensor response into the number of moles of Hg desorption from each surface.

Hg sorption isotherms (see Supporting Information, Figure S4) that the Hg−Au adsorption better fits a linear type adsorption isotherm at room temperature and transforms to a Freundlich type at ∼100 °C before showing a Langmuir type behavior at temperatures above 100 °C. The data in Figure 5a also demonstrate that the surface area difference between the two surfaces is not the reason for the higher response magnitude of the Au-rough compared to that of the Au-polished surface, as it would have otherwise been expected that the ratio of Hg sorption between the two surfaces be constant at all the tested operating temperatures. To demonstrate the effect of ESA on Hg sorption, the Hg sorption of the Au-rough and Au-polished films (derived from data in Figure 5a) were normalized for their ESA and presented in Figure 5b. The Au-rough film is clearly observed to have a lower Hg sorption capacity following 1 h exposure to Hg (observed for all Hg concentrations) at all operating temperatures tested, when accounting for the ESA of each film. The difference in Hg sorption capacity between the two Au films becomes more obvious at the higher operating temperature, with the Au-polished QCM having ∼140% higher Hg sorption at 132 °C compared to 15% at 28 °C when compared to the Au-rough QCM at the respective operating temperatures. However, after accounting for the ESA, the Au-rough sample shows a Hg sorption capacity lower than that of the Au-polished surface. On the basis of the findings of Steckel et al.[42] that Hg binding is stronger on the (001) face than on the (111) face of the Au surface, we postulate that the difference in Hg sorption capacity is likely due to the difference in the films' crystallography features of the two surfaces (XRD shown in Figure 2). That is, the Hg sorption capacity difference between the two films at the various operating temperatures is due to the exposed crystallographic planes on the surface and not due to any surface morphology changes occurring as a result of the change in temperatures.

3.3.1. Hg Sorption and Desorption Model. A better understanding of Hg sorption and desorption kinetics from Au-rough and Au-polished films may be achieved if the Hg sorption and desorption rates (k) and E_a are calculated as a function of time $\{k(t)$ and $E_a(t)\}$ during the Hg exposure and recovery periods of the sensor. To do this, the Hg sorption and desorption kinetics needs to be modeled as a function which would hold true for all operating temperatures and Hg vapor concentrations. Previously, Drelich et al.[43] have shown that cantilevers can be used to estimate the amount of Hg adsorbed on optically polished Au surfaces as a function of time at room temperature and proposed the model $\Delta m = Bt^n$ (where B and n are constants). Although the function fitted well with most of their experimental data points (R^2 value was not reported), we found that it had a very poor fit to our data. This may be due to our experimental conditions having up to 2 orders of magnitude higher Hg vapor concentrations and operating temperatures above 21 °C, for which the function was proposed. However, it was found that for our data, the 60 min Hg sorption and desorption from Au surfaces were best described by the rational function in eq 2 with the coefficient of determination (R^2) above 0.998 for every operating temperature and Hg concentration tested.

$$\Delta f(t) = \frac{P(t)}{Q(t)} \tag{2}$$

The parameter $\Delta f(t)$ is the sensor response toward Hg vapor as a function of time while $P(t)$ and $Q(t)$ are one-degree polynomial expressions in time (where $Q(t) \neq 0$). After accounting for the ESA of each film, an expression for the amount of Hg ($n_{Hg}(t)$) undergoing sorption or desorption from the sensor surface during Hg exposure and recovery phases, respectively, can be formulated by combing eq 1 with eq 2:

$$n_{Hg}(t) = \frac{b + ct}{a + t}, \text{ with } 0 \leq t \leq 60 \text{ and } a > 0 \text{ min} \tag{3}$$

where the constants a, b, and c are dependent on temperature, having units of min, mol·min, and mol, respectively. The parameter t is the Hg exposure or sensor recovery time. The parameters a, b, and c for the different conditions are given in Table 1 and are all observed to generally decrease with increasing operating temperature. The constant a gives an indication of the Hg sorption and desorption kinetics with values closer to zero representing the faster kinetics. The extent of Hg sorption or amalgamation to the Au-sensitive layer from previous Hg exposures is determined by the value of b with the least value of zero representing an Au surface having had no prior exposure to Hg. The maximum Hg sorption capacity during the exposure period or maximum amount of Hg that can be removed during the sensor recovery period is determined from the c value. The higher the c value, the better the Hg vapor sensors' sensitivity or recovery characteristics. The ratio of b/a represents the amount of Hg accumulated on the surface from prior Hg exposure events. Therefore, the model in eq 3 accounts for any accumulated Hg vapor on the sensor from earlier events at any constant operating temperature. In addition, eq 3 fits well for both sorption and desorption parts of the QCM response curves at any operating temperature as demonstrated in Figure 6.

3.3.2. Hg−Au Sticking Probability. To observe and compare the affinity of the Au-polished and Au-rough surfaces toward Hg vapor, the sticking probability (S) was calculated at the different

dx.doi.org/10.1021/jp2091895 |J. Phys. Chem. C 2012, 116, 2483–2492

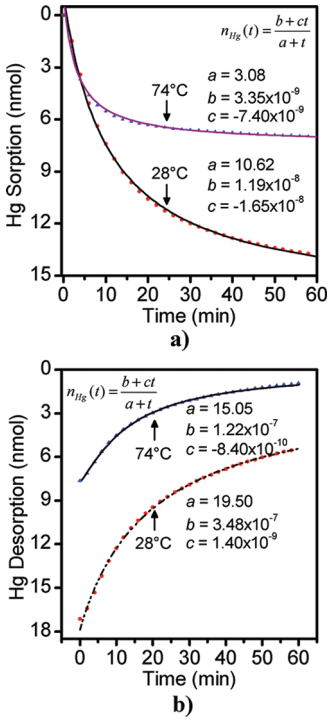

Figure 6. Results of Au-rough QCM response data (symbols) and fitted (solid lines) curve using eq 3 during (a) Hg sorption and (b) Hg desorption periods when the QCM was exposed to a Hg vapor concentration of 5.70 mg/m^3 at operating temperatures of 28 °C and 74 °C. The sensor response has been converted to moles of Hg vapor undergoing sorption and desorption while accounting for the ESA.

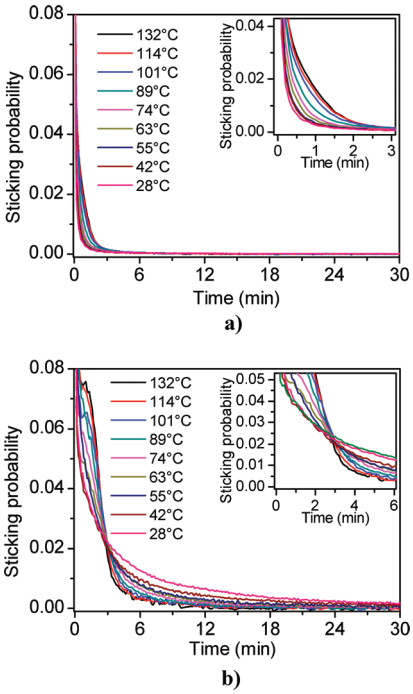

Figure 7. Sticking probability for (a) Au-polished and (b) Au-rough surfaces for operating temperatures between 28 °C to 132 °C.

operating temperatures tested. Sticking probability is defined as the ratio of the rate of sorption (K_{ads}) to the rate at which atoms from the vapor phase strike the surface (Z_W).[24] The K_{ads} parameter was estimated from the Hg sorption/desorption expression in eq 3. The S profiles of both Au surfaces exposed to a pulse of Hg vapor at a concentration of 5.70 mg/m^3 at various operating temperatures is shown in Figure 7. It can be observed from Figure 7a that the sticking probability on the Au-polished QCM decreases significantly, reaching from one to a value close to zero in the first 2 to 3 min of exposure to Hg at all the operating temperatures tested. From the inset in Figure 7a, however, we observe a trend where the affinity of the Au-polished toward Hg increases in the first 2 to 3 min as the operating temperature is increased. In Figure 7b it is observed that the Au-rough QCM also has a similar affinity toward Hg especially at higher operating temperatures; however, the trend is observed to reverse following a 2−3 min period of exposure to Hg. After considering the ESA difference between the two surfaces, the Au-rough QCM appeared to maintain a higher affinity toward Hg and for a longer period of time relative to Au-polished at every operating temperature. The S value is dependent on factors such as the collision rate of the gaseous atoms with the solid surface, the probability of finding a suitable site, the probability of being in correct orientation, and the probability of overcoming the adsorption barrier.[44] The parameters that influence the affinity of Au toward Hg are the solubility of Au in Hg and wetting characteristics of Hg on Au surfaces,[45] both of which increase with increasing temperature.[46−48] The other parameter is the change in the vapor pressure of Hg with temperature. That is, at increasing operating temperatures, the amount of Hg that can be saturated in air increases, reducing the tendency of Hg atoms to adsorb on the Au surface. This parameter becomes the repulsion rather than the affinity parameter with increasing operating temperatures. Depending on the operating temperature, the affinity and repulsion parameters mentioned would compete, resulting in the different temperature profiles for each surface, as observed in Figure 5. Note also that the increase in temperature also increases the gas atoms' kinetic energy, resulting in their reduced tendency to adsorb/amalgamate on the surface.[44] Under such conditions, surfaces with a large number of kinks, edges, and other defects are required for the Hg vapor atoms to collide and lose their kinetic energy, resulting in Hg sorption, amalgamation, and diffusion.[44]

3.3.3. Hg Diffusion and Accumulation in Au Thin-Films. Following Hg adsorption on the Au thin-films, the Hg atoms are thought to accumulate at Hg sorption sites on the film surface prior to undergoing diffusion into the Au bulk. To better understand the diffusion behavior of Hg in Au films, a specially designed ultrathin Au film (40 nm)-based QCM was fabricated and exposed to Hg vapor prior to characterization using SIMS depth profiling (refer to experimental section 2.1). The sensor response and the SIMS depth profiles of the 40 nm ultrathin Au surfaces (unexposed as well as Hg exposed) are shown in Figure 8. It can be observed from Figure 8a that the response profile of the 40 nm Au ultrathin film-based QCM fails to reach saturation even after 14 h of exposure to Hg. This is evidence of continuous Hg diffusion in the Au film and release of Hg sorption sites on the surface for more Hg to undergo sorption process, which is in line with previous reports.[21,26] Further evidence is shown by the SIMS depth profiling data in Figure 8b and 8c for the control and Hg-exposed Au ultrathin films, respectively. The existence of the "hump" (as indicated in Figure 8c) in the Hg profile is observed to occur at the depth corresponding to the interface between the Au film and SiO_2 layers (Au/SiO_2 interface) of the Hg-exposed

dx.doi.org/10.1021/jp2091895 |J. Phys. Chem. C 2012, 116, 2483–2492

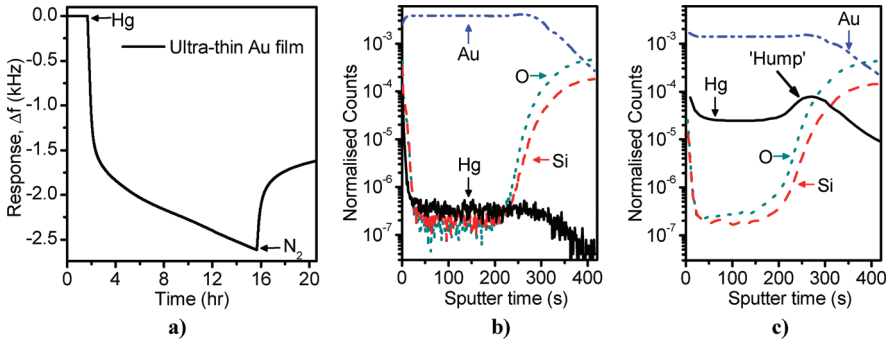

Figure 8. (a) QCM response of Au-based ultrathin film (40 nm) exposed to 10.55 mg/m^3 of Hg at 28 °C for 14 h followed by 5 h recovery under nitrogen atmosphere, all at a constant flow rate of 200 sccm. The SIMS depth profile of (b) Au ultrathin control with no Hg exposure and (c) Au ultrathin film exposed to Hg as shown in panel a.

Au ultrathin film. This hump is not observed for the unexposed sample (Figure 8b), confirming that Hg diffuses right through the 40 nm Au thin-film and accumulates at the Au/SiO_2 interface. The accumulation of Hg at Au/SiO_2 interfaces have been observed previously by Be'er et al.[49,50] where a drop of Hg (in liquid form) was placed on a thin film of Au and was observed to diffuse in the film until reaching the Au/SiO_2 interface. Such Hg accumulations may be the reason for the high temperatures of 150−700 °C[17−19] reported to be required for recovering (full desorption) Au films following Hg-exposure events.

3.3.4. Desorption Kinetics. To better understand Hg desorption (sensor recovery) from the Au-polished and Au-rough films, the $E_a(t)$ for each film was evaluated from the QCM response data obtained during the nitrogen recovery period following each Hg exposure. The $E_a(t)$ for Hg desorption was evaluated by using Arrhenius equation, eq 4:

$$\ln[k(t)] = \ln[A(t)] - \frac{E_a(t)}{RT} \quad (4)$$

where A is the pre-exponential factor,[51] T is the operating temperature (K), R is the ideal gas constant ($8.3144\,J^{-1}\cdot K^{-1}\cdot mol^{-1}$), and $k(t)$ is the Hg sorption or desorption rate from the thin Au film as a function of time. For a first-order ($n = 1$) desorption kinetic, $k(t)$ may be estimated by evaluating the derivative of the logarithm of eq 3) as shown in eq 5):

$$k(t) = \frac{\partial}{\partial t}\langle \ln[n_{Hg}(t)]\rangle = (ca - b)/[(a + t)(b + ct)] \quad (5)$$

Subsequently, for a second-order desorption kinetics or higher ($n \geq 2$), $k(t)$ may be estimated by eq 6:

$$(n-1)k(t) = \frac{\partial(1/n_{Hg})^{n-1}}{\partial t} \Longrightarrow k(t)$$

$$= -\frac{(ca - b)(a + t)^{n-2}}{(b + ct)^n} \quad (6)$$

The logarithmic value of k or $\ln(k)$ at each time point may then be plotted against $1/T$ (Arrhenius plot) for the subsequent estimation of E_a (as in eq 4)) from the slope of the Arrhenius plot. This step may be performed for all t to observe the change in E_a during the recovery period, $E_a(t)$.

In this study, the above calculations were performed for different values of n, and the Hg sorption/desorption order was selected when the summation of all the R^2 values for each time point during the 60 min Hg sorption or desorption period was at its maximum value. Understandably, due to the unique temperature profiles shown in Figure 5 (which was observed to be similar to Hg desorption profiles), the derived Arrhenius plot was found to be nonlinear. Consequently, two separate temperature ranges were found to produce linear Arrhenius plots between the ranges of 55−101 °C and 28−74 °C for both the Au-rough and Au-polished QCMs. In each of the temperature ranges, an R^2 value >0.99 was calculated throughout all the 60 min recovery periods. The fact that a different range of the temperature profile data (especially for the case of the Au-polished surface) could be used to evaluate different values for the activation energy indicates either (i) the presence of a variety of adsorption sites with different desorption activation energies, (ii) that adsorption has occurred on different crystal planes where some may have higher affinity for Hg than others, (iii) that activation energy is dependent on the extent of Hg coverage on the Au surface, and/or (iv) that multilayer adsorption has occurred where Hg desorbing from a Hg layer would require less energy than amalgamated Hg desorbing from an Au film.

Because the chemisorption of Hg to the Au surface is a nonactivated process and there is no dissociation involved (Hg is monatomic), the activation energy for desorption can be interpreted in terms of the adsorption enthalpy which must be negative (exothermic) due to the spontaneous sorption process of Hg on Au as observed in Figure 3d. However, Hg desorption from the Au thin-films is known to be an activated process due to the chemisorption nature of Hg on Au and thus typically requires either high temperature or acid dissolution[31] to remove most of the Hg from the Au surface.

To understand how Hg desorption kinetics change as the Hg surface coverage on gold decreases during the recovery period, the activation energy during the 60 min desorption period for both the Au-polished and Au-rough surfaces were evaluated using eq 6. $E_a(t)$ is shown in Figure 9a which was evaluated from the desorption constants a, b, and c (given in Table 1) obtained following a Hg pulse of 5.7 mg/m^3. It was found that high R^2 values were obtained when Hg desorption kinetics from Au surfaces were adjusted to be a second-order process ($n = 2$). However, a first-order desorption process ($n = 1$) was found to be a better representation (R^2 values closer to 1) for the first 10 min Hg desorption period from the Au-polished surface having a reasonably constant E_a of ∼15 kJ/mol as observed in Figure 9b. From the QCM response magnitude, it was calculated that depending on the operating temperature, ∼0.5 to 1.5 nominal monolayers (ML) of Hg remains on the surface at the 10 min recovery mark.

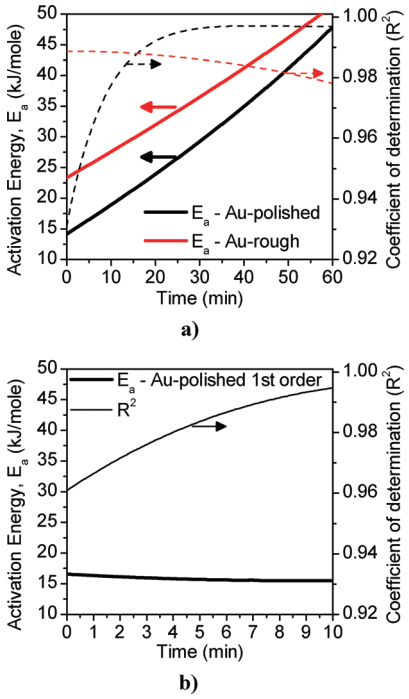

Figure 9. Desorption E_a of (a) Au-polished for temperature range of 55−101 °C and Au-rough surface for temperature range of 28−74 °C treated as a second-order kinetic and (b) Au-polished surface for temperature range 55−101 °C treated as a first-order kinetic.

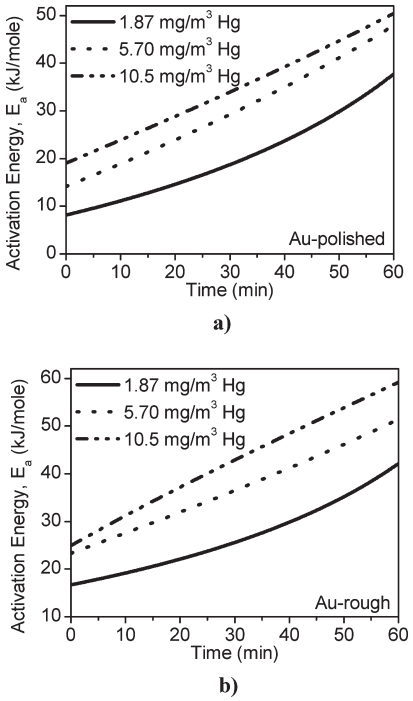

Figure 10. Desorption E_a of (a) Au-polished and (b) Au-rough surfaces at different Hg concentrations.

This indicates that potentially two different processes were occurring during the Hg desorption period of the experiment. In the initial phase, the less strongly bound Hg atoms above the first Hg layer were removed, leaving the more tightly bound Hg atoms directly attached or diffused into the Au surface behind. The desorption kinetics are first order in mercury coverage with an activation energy equal to the heat of adsorption ΔH_{ads} ~15 kJ/mol. Thereafter, the amalgamated/diffused Hg atoms, which require more energy to desorb from the Au surface, are expected to desorb from the Au surface. This second step is observed in Figure 9a where the E_a is shown to increase with increasing recovery time or reduced Hg coverage. The increase in desorption activation energy and the fact that it fits well in a second-order kinetic indicates that two separate conditions need to be satisfied before Hg desorption from the Au surface can occur. That is, mercury atoms first need to detach from the Hg sorption sites and migrate across the Au surface undergoing full desorption. As the Hg detaches from the Hg sorption site, the diffused Hg from the bulk may then migrate back to the surface where further Hg detachment and desorption process may occur, agreeing well with the requirement of long recovery times and increasing activation energy as a function of recovery time observed in Figure 9b.

The process of desorption described is the reverse of those proposed for Hg sorption on Au films where Hg first becomes mobile on the Au surface until it reaches a Hg sorption site such as a surface defect or grain boundary[21,25] before diffusing rapidly via place exchange mechanism.[26] This process is said to occur at a rapid rate, resulting in mercury accumulation above one nominal monolayer, without a continuous monolayer formation ever being observed on the Au film surface.[26,52] The results observed in Figure 9 agree well with similar results obtained by Jones et al.[53] in the case of the Hg−Fe system where it was proposed that there may be an activation energy which increases as the Hg coverage on the surface decreases (or with increasing recovery time in this case).

A comparison of the desorption kinetics between the Au-rough and Au-polished surfaces revealed that the desorption E_a for Au-rough surface is higher than that of the Au-polished surface during the total desorption period when accounting for the ESA difference between the two surfaces. This suggests that the larger number of surface defect sites on the Au-rough film, which acts as Hg sorption sites,[21,54] more tightly bind the Hg atoms to the surface. Evidence of this can be confirmed by comparing the Arrhenius pre-exponential value (A) for the Au-polished surface during the recovery period, which increased from 3.08×10^7 to 5.50×10^{12} mol·cm^{-2}·min^{-1} at 60 min, confirming that the less mobile Hg atoms are removed toward the end of the 60 min recovery period. In comparison, the A values of Au-rough increased from 4.66×10^8 to 2.04×10^{13} mol·cm^{-2}·min^{-1}, indicating that the Hg atoms are bound tighter to the Au-rough film than to the Au-polished film.

To study the amount of initial Hg exposure and its effect on the desorption kinetics, the desorption E_a values was calculated for both surfaces over the 60 min recovery period following 60 min of exposure to Hg at different concentrations, as shown in Figure 10. It is observed that the higher the initial Hg vapor concentration during exposure, the higher the required desorption activation energy at any stage during the recovery period in the cases of both Au-polished and Au-rough surfaces. Theoretically, a relatively higher activation energy is required to remove the more enriched amalgams, as they require higher energies to be formed compared to an adsorbed Hg atom on Au films.[26] Previous studies undertaken by Inukai et al.[52] also show that Hg amalgamation on Au occurred following bulk Hg deposition. Gold is also well-known to have low solubility in elemental mercury[55] with past literature suggesting that the high affinity of Hg to Au is due to its wetting ability.[45,50] However, wetting of Au by Hg vapor

dx.doi.org/10.1021/jp2091895 |J. Phys. Chem. C 2012, 116, 2483–2492

may occur when enough Hg atoms come into close proximity on a surface, changing the Hg cluster from a Van der Waals (nonmetal) modification to a metallic modification.[56−58] These past findings indicate that a certain number of Hg atoms need to be collected at the active sorption sites on the Au surface before any wetting and amalgamation processes can occur. Therefore, our observation that an exposure to a higher concentration of Hg increases the required desorption activation energy during the recovery period for both Au-polished and Au-rough surfaces agrees well with these past findings. Furthermore, our findings demonstrate how Au surfaces with different morphologies can be used, depending on whether the application is for Hg monitoring where a high recovery rate is desired, or for Hg removal applications where a higher Hg sorption and/or retention rates are required.

4. CONCLUSIONS

In this study, the Hg sorption/desorption kinetics from Au thin-films were experimentally obtained by using the relationship between QCM response and mass sorption/desorption following Hg exposure of the Au films under controlled conditions. The sorption and desorption kinetics of Hg from Au surfaces were found to be best described by the rational function with $R^2 > 0.998$ for all tested operating temperature and Hg concentrations. The activation energy was calculated as a function of time $\{E_a(t)\}$ using the rational functions fitted to the QCM response curves during the recovery period following the exposure to Hg vapor at eight different operating temperatures ranging from 28 °C to 132 °C. It was observed that the Hg desorption activation energy $E_a$increased as the surface Hg coverage on the Au thin-films was decreased. When comparing two different surface morphologies, it was found that the optically polished Au film had a higher Hg capacity following 1 h of exposure to Hg as well as a lower Hg desorption E_a compared to those of the mechanically roughened Au film. Furthermore, it was observed that the Au deposited on optically polished and mechanically roughened QCM crystals exhibited cubic and asymptotic type temperature profiles, respectively, indicating differing Hg sorption kinetics between the two surface types at different operating temperatures. The Hg sorption temperature profile difference between the two surfaces was attributed to the difference in Hg−Au sticking probability profiles of the two surfaces at different operating temperatures as well as the difference in crystallographic orientation of the two surfaces, as shown by the XRD analysis. It was also found that Hg vapor underwent diffusion through the Au films and accumulated at the Au/SiO_2 interface. Gold thin-films deposited on mechanically roughened substrates are best used as Hg collectors as Hg diffuses through the film and requires relatively higher E_a to desorb. On the other hand, Au deposited on an optically polished substrate would best be used for Hg monitoring applications because of its higher capacity per surface area as well as a lower E_a requirement when undergoing a recovery process. Therefore, the crystal plane exposed at the surface of the film and the surface morphology of the Au film are critical properties to consider when developing materials for Hg monitoring and removal applications.

■ ASSOCIATED CONTENT

Ⓢ Supporting Information. Figure S1: AFM images of (a) Au-polished and (b) Au-rough prior to being exposed to Hg vapor. Figure S2: Hg sorption isotherms of Au-polished with Au film thicknesses of either 100, 150, or 200 nm when exposed to a Hg concentration of 10.55 mg/m^3 at operating temperatures ranging between 28 °C and 175 °C. Figure S3: QCM response of Au-polished with Au film thicknesses of 50, 150, and 200 nm exposed to a Hg concentration of 10.55 mg/m^3 at an operating temperature of ∼90 °C. Figure S4: Hg sorption isotherms of (a) Au-polished and (b) Au-rough exposed to five different Hg concentrations ranging from 1.02 to 10.55 mg/m^3 at operating temperatures between 28 °C and 132 °C. This material is available free of charge via the Internet at http://pubs.acs.org.

■ AUTHOR INFORMATION

Corresponding Author

*E-mail: suresh.bhargava@rmit.edu.au (S.K.B.), samuel.ippolito@rmit.edu.au (S.J.I.). Phone: +61 3 9925 2330.

■ ACKNOWLEDGMENT

We acknowledge the Australian Research Council (ARC) for supporting this project (grant number LP100200859) and the RMIT microscopy and microanalysis facility (RMMF) for allowing the use of their comprehensive facilities and services. The authors acknowledge the support from the Australian Institute of Nuclear Science and Engineering (AINSE) for providing access to SIMS under an AINSE grant (AINGRA08104P).

■ REFERENCES

(1) Goldman, R. L.; Shannon, M. W. *Pediatrics* **2001**, *108*, 197.
(2) Baughman, T. A. *Environ. Health Perspect.* **2006**, *114*, 147.
(3) Rong, Y.; David Tee, L.; Joo Hwa, T. *Environ. Sci. Pollut. Res. Int.* **2003**, *10*, 399.
(4) Reisch, M. *Business* **2008**, *86*, 22.
(5) Selid, P.; Xu, H.; Collins, E. M.; Striped Face-Collins, M.; Zhao, J. X. *Sensors* **2009**, *9*, 5446.
(6) Johnson, N. C.; Manchester, S.; Sarin, L.; Gao, Y.; Kulaots, I.; Hurt, R. H. *Environ. Sci. Technol.* **2008**, *42*, 5772.
(7) Guminski, C. *J. Less-Common Met.* **1991**, *168*, 329.
(8) McNerney, J. J.; Buseck, P. R.; Hanson, R. C. *Science* **1972**, *178*, 611.
(9) Granite, E. J.; Pennline, H. W.; Hargis, R. A. *Ind. Eng. Chem. Res.* **2000**, *39*, 1020.
(10) Braman, R. S.; Johnson, D. L. *Environ. Sci. Technol.* **1974**, *8*, 996.
(11) Yan, T. Y. *Ind. Eng. Chem. Res.* **1994**, *33*, 3010.
(12) Diggs, T. H.; Ledbetter, J. O. *Am. Ind. Hyg. Assoc. J.* **1983**, *44*, 606.
(13) Reed, C. E.; Kanazawa, K. K.; Kaufman, J. H. *J. Appl. Phys.* **1990**, *68*, 1993.
(14) Dumarey, R.; Dams, R.; Hoste, J. *Anal. Chem.* **1985**, *57*, 2638.
(15) Sabri, Y. M.; Kojima, R.; Ippolito, S. J.; Wlodarski, W.; Kalantar-zadeh, K.; Kaner, R. B.; Bhargava, S. K. *Sens. Actuators, B* **2011**, *160*, 616.
(16) Sabri, Y. M.; Ippolito, S. J.; O'Mullane, A. P.; tardio, J.; Bansal, V.; Bhargava, S. *Nanotechnology* **2011**, *22*, 305501.
(17) Schroeder, W. H.; Hamilton, M. C.; Stobart, S. R. *Rev. Anal. Chem.* **1985**, *8*, 179.
(18) Scheide, E. P.; Taylor, J. K. *Am. Ind. Hyg. Assoc. J.* **1975**, *36*, 897.
(19) Schweyer, M. G.; Andle, J. C.; McAllister, D. J.; Vetelino, J. F. *Sens. Actuators, B* **1996**, *35*, 170.
(20) Zierhut, A.; Leopold, K.; Harwardt, L.; Worsfold, P.; Schuster, M. *J. Anal. At. Spectrom.* **2009**, *24*, 767.
(21) George, M. A.; Glaunsinger, W. S. *Thin Solid Films* **1994**, *245*, 215.
(22) Sabri, Y. M.; Ippolito, S. J.; Tardio, J.; Sood, D. K.; Bhargava, S. K. Electro-deposition of gold nano-structures on gold Quartz Crystal Microbalance (QCM) electrodes for enhanced mercury vapour sensitivity

in the presence of interferent gases. Presented at the International Conference on Nanoscience and Nanotechnology (ICONN), Melbourne, Australia, Feb 25−29, 2008.
(23) Sawant, P. D.; Sabri, Y. M.; Ippolito, S. J.; Bansal, V.; Bhargava, S. K. *Phys. Chem. Chem. Phys.* **2009**, *11*, 2374.
(24) Sabri, Y. M.; Ippolito, S. J.; Tardio, J.; Atanacio, A. J.; Sood, D. K.; Bhargava, S. K. *Sens. Actuators, B* **2009**, *137*, 246.
(25) George, M. A.; Glaunsinger, W. S.; Thundat, T.; Lindsay, S. M. *J. Microsc.* **1988**, *152*, 703.
(26) Levlin, M.; Ikavalko, E.; Laitinen, T. *Fresenius J. Anal. Chem.* **1999**, *365*, 577.
(27) Morris, T.; Szulczewski, G. *Langmuir* **2002**, *18*, 2260.
(28) Schoettel, G.; Vittal, J. J.; Puddephatt, R. J. *J. Am. Chem. Soc.* **1990**, *112*, 6400.
(29) Fialkowski, M.; Grzeszczak, P.; Nowakowski, R.; Holyst, R. *J. Phys. Chem. B* **2004**, *108*, 5026.
(30) Li, J.; Abruna, H. D. *J. Phys. Chem. B* **1997**, *101*, 2907.
(31) Morris, T.; Sun, J.; Szulczewski, G. *Anal. Chim. Acta* **2003**, *496*, 279.
(32) Caron, J. J.; Haskell, R. B.; Benoit, P.; Vetelino, J. F. *IEEE Trans. Ultrason., Ferroelect., Freq. Control* **1998**, *45*, 1393.
(33) Scheide, E. P.; Taylor, J. K. *Environ. Sci. Technol.* **1974**, *8*, 1097.
(34) Wu, Y.-T.; Akoto-Ampaw, P.-J.; Elbaccouch, M.; Hurrey, M. L.; Wallen, S. L.; Grant, C. S. *Langmuir* **2004**, *20*, 3665.
(35) Buttry, D. A.; Ward, M. D. *Chem. Rev.* **1992**, *92*, 1355.
(36) Ward, M. D.; Buttry, D. A. *Science* **1990**, *249*, 1000.
(37) O'Sullivan, C. K.; Guilbault, G. G. *Biosens. Bioelectron.* **1999**, *14*, 663.
(38) Tsionsky, V.; Gileadi, E. *Langmuir* **1994**, *10*, 2830.
(39) Laudal, D.; Nott, B.; Brown, T.; Roberson, R. *Fresenius' J. Anal. Chem.* **1997**, *358*, 397.
(40) Rand, D. A. J.; Woods, R. *J. Electroanal. Chem.* **1971**, *31*, 29.
(41) Raffa, V.; Mazzolai, B.; Mattoli, V.; Mondini, A.; Dario, P. *Sens. Actuators, B* **2006**, *114*, 513.
(42) Steckel, J. A. *Phys. Rev. B: Condens. Matter Mater. Phys.* **2008**, *77*, 115412.
(43) Drelich, J.; White, C. L.; Xu, Z. *Environ. Sci. Technol.* **2008**, *42*, 2072.
(44) Atkins, P. W. *Physical Chemistry*, 2nd ed.; Oxford University Press: Oxford, Great Britain, 1982.
(45) Brown, J. B. *J. Chem. Educ.* **1960**, *37*, 415.
(46) Sunier, A. A.; White, C. M. *J. Am. Chem. Soc.* **1930**, *52*, 1842.
(47) Anderson, J. T. *J. Phys. Chem.* **1932**, *36*, 2145.
(48) Britton, G. T.; McBain, J. W. *J. Am. Chem. Soc.* **1926**, *48*, 593.
(49) Be'er, A.; Lereah, Y.; Taitelbaum, H. *Mater. Sci. Eng., A* **2008**, *495*, 102.
(50) Be'er, A.; Lereah, Y.; Frydman, A.; Taitelbaum, H. *Phys. A (Amsterdam, Neth.)* **2002**, *314*, 325.
(51) Tagawa, M.; Yokota, K.; Kida, T.; Ohmae, N. Temperature and Impingement Angle Dependences of Atomic Oxygen-Induced Erosion of Polyimide and Polyethylene Films Measured by Quartz Crystal Microbalance. In *Protection of Materials and Structures from Space Environment*; Kluwer Academic Publishers: Dordrecht, Netherlands, 2004; p 391.
(52) Inukai, J.; Sugita, S.; Itaya, K. *J. Electroanal. Chem.* **1996**, *403*, 159.
(53) Jones, R. G.; Perry, D. L. *Vacuum* **1981**, *31*, 493.
(54) Green, T. A. *Gold Bull.* **2007**, *40*, 105.
(55) Guminski, C.; Galus, A.; Hirayama, C. International Union of Pure and Applied Chemistry (IUPAC). In *Solubility Data Series: Metals in Mercury*; Warsaw, U. O., Ed.; Pergamon Press: Warsaw, Poland, 1986; Vol. 25, p 258.
(56) Mott, N. F. *Philos. Mag.* **1961**, *6*, 287.
(57) Miedema, A. R.; Dorleijn, J. W. F. *Philos. Mag. B* **1981**, *43*, 251.
(58) Jansen, H. J. F.; Freeman, A. J.; Weinert, M.; Wimmer, E. *Phys. Rev. B* **1983**, *28*, 593.